BMC Microbiology

RESEARCH

Open Access

Two virulent *Vibrio campbellii* phages with potential for phage therapy in aquaculture

Huiyu Ding[1,2], Keming Shi[2,3], Min Hsiao[4], Wenqing Li[2,3], Xin Liu[1,2], Jie Xu[5], Yunlan Yang[6*] and Rui Zhang[6*]

Abstract

Background As aquaculture continues to expand globally, diseases caused by *Vibrio* species are becoming increasingly prevalent. Vibriosis encompasses a range of infections, which can lead to symptoms such as skin lesions, hemorrhaging, and high mortality rates in fish and shellfish, especially in high-density farming systems, resulting in significant economic losses. Simultaneously, the extensive use of antibiotics has fostered the emergence of antibiotic-resistant bacteria, exacerbated disease outbreaks, and complicated control measures. Phage therapy, which leverages bacteriophages as natural antibacterial agents, offers a promising eco-friendly alternative to the antibiotics used in aquaculture. This study aimed to evaluate the potential of two vibriophages for phage therapy in aquaculture.

Results Two virulent vibriophages, vB_VcaP_R24D and vB_VcaP_R25D, were isolated from aquaculture wastewater from seafood markets using *Vibrio campbellii* LMG 11216^T as the host strain. The two vibriophages were identified based on their morphology, infection dynamics, host range, genomic features, lytic activity, and environmental stability. Both phages belong to the podovirus morphotype and exhibit a lytic life cycle characterised by a short latent period (< 10 min). Genomic analyses confirmed the absence of lysogenic genes, virulence factors, and antibiotic-resistance genes, thereby ensuring genetic safety. Additionally, both phages demonstrated high stability over a broad range of temperatures (4–45 °C) and pH (3–10). Lytic curve analyses further indicated a robust lytic efficiency during the logarithmic growth phase of the vibriophages.

Conclusions These biological and genomic characteristics highlight the potential of vB_VcaP_R24D and vB_VcaP_R25D as effective biocontrol agents for mitigating vibriosis in aquaculture. Although this study demonstrates their narrow host range, the possibility of phage infection in other untested hosts cannot be entirely excluded. Furthermore, the findings offer valuable insights for future research on phage-host interactions and the development of phage cocktails to improve disease management in aquaculture systems.

Keywords *Vibrio*, Vibriophage, Phage therapy, Aquaculture

*Correspondence:
Yunlan Yang
yangyunlan@szu.edu.cn
Rui Zhang
ruizhang@szu.edu.cn

Full list of author information is available at the end of the article

Background

The global fishery and aquaculture production reached a record high of 223.2 million tons in 2022, with aquaculture production of animal species surpassing that of capture fisheries for the first time (FAO, 2024). As the global demand for seafood increases, the aquaculture industry has expanded rapidly, with high-density, large-scale, and intensive farming practices becoming increasingly prevalent. However, the increasing incidence of aquatic animal diseases, with bacterial infections representing the most frequent type of infectious disease in aquaculture. In particular, diseases caused by *Vibrio* species are increasing, posing significant challenges to the development of aquaculture industry [1–3].

Vibrio, a genus of halophilic Gram-negative bacteria commonly found in estuarine and coastal ecosystems, is classified as an opportunistic pathogen [4]. Common pathogenic *Vibrio* species include *V. cholerae*, *V. alginolyticus*, *V. parahaemolyticus*, *V. campbellii*, and *V. harveyi*. Several reports have highlighted various diseases caused by *Vibrio* species in aquaculture, such as lethal hepatopancreatic septic necrosis and acute hepatopancreatic necrosis disease (AHPND), both of which have caused significant damage to shrimp farming worldwide [5–7]. Additionally, *V. alginolyticus* is linked to Zoea II Syndrome, which causes significant mortality in whiteleg shrimp owing to impaired moulting. Although studies on the pathogenicity of *V. campbellii* are relatively limited, existing research has demonstrated its potential to cause diseases, such as luminescent vibriosis and AHPND. For instance, Dong et al. isolated a *V. campbellii* strain (20130629003S01) from a shrimp farm, which carried the pir^{vp} gene; shrimp immersed in this strain suspension developed typical AHPND symptoms within 12 h, with a cumulative mortality rate of 100% within 36 h, indicating a high virulence. Similarly, Haldar et al. isolated 26 *V. campbellii* strains from diseased shrimp, and infection experiments using *Artemia* as a model revealed that eight strains exhibited high pathogenicity and three strains showed moderate pathogenicity, and the pathogenic strains were capable of colonising the *Artemia* gut within 24 h. These findings underscore the significant pathogenic potential of *V. campbellii* and warrant more attention in aquaculture disease management [8–11]. The extensive use of antibiotics has led to adverse impacts on environmental health, ecological stability, public health, and food safety [12, 13]. Consequently, there is an urgent demand for sustainable and effective alternatives to antibiotics [14–16]. Bacteriophages, as natural antimicrobial agents, are capable of specifically and efficiently lysing bacterial hosts, making them a microbiologically and environmentally sustainable solution. Bacteriophages have shown substantial potential in mitigating *Vibrio* infections in aquaculture [17, 18]. Recent studies have isolated various vibriophages and evaluated their biological and genomic characteristics to assess their potential for controlling vibriosis in aquaculture [19, 20]. Phage lytic ability, bactericidal efficiency, and environmental stability are key factors determining the application potential and suitability of phage cocktail formulations. In aquaculture, the absolute lytic capability of a phage is essential for its application as it ensures efficient pathogen elimination without entering a lysogenic state, thus preventing horizontal gene transfer and reducing the risk of antibiotic resistance [21]. The bactericidal efficacy of a phage is another critical measure of its therapeutic potential. For instance, a phage against *V. parahaemolyticus* was isolated from a shrimp farm in India, and its one-step growth and bactericidal curves demonstrated high lytic activity against the host bacterium (burst size of 2.9×10^8 PFU mL^{-1}, with the optical density (OD_{600}) value of the phage-treated group consistently below 0.2). In infection experiments, the survival rate of shrimp treated with this phage significantly increased [22]. The environmental stability of phages is a key criterion for their production, marketing, and practical applications. The *V. alginolyticus* phage vB_Va_Val-yong3 was isolated and shown to be stable under various conditions, possessing features such as resistance to chloroform resistance, relative UV tolerance, and stability across a temperature range of 4–50 °C and pH range of 5–12. In a phage treatment experiment, the survival rate of mud crab larvae increased from 33.33 to 51.67% after treatment with vB_Va_Val-yong3 [23].

This study aimed to investigate the vibriophage potential of two novel lytic phages, vB_VcaP_R24D and vB_VcaP_R25D, isolated from wastewater of a seafood market in Xiamen using the type strain *V. campbellii* LMG 11216^T as the host. Comprehensive characterization of these phages revealed their strong lytic activity, supported by detailed analyses of their morphological features, infection kinetics, host range specificity, genomic composition, phylogenetic relationships, taxonomic placement, and environmental stability. Moreover, phage co-infection kinetics analysis revealed their individual and synergistic bactericidal capabilities, highlighting their efficacy in controlling *V. campbellii*. This is the first study to isolate such potent lytic phages targeting *V. campbellii* from aquaculture environments and systematically evaluate their combined bactericidal effects. These findings offer significant insights into the application of phage therapy as a sustainable strategy for managing vibriosis in aquaculture.

Methods

Phage isolation and purification

In this study, *V. campbellii* LMG 11216^T, a strain obtained from the Belgian Coordinated Collection of

Microorganisms, was used as a host for phage isolation. The strain was cultured in 2216E liquid medium (10 M tryptone, 2 M yeast extract, and artificial seawater, pH 7.5) at 28 °C with shaking at 160 rpm min^{-1}. In July 2023, water samples were collected from the wastewater pipelines of Bashi (118.07°E, 24.46°N) and Xiashang (118.10°E, 24.55°N) seafood markets in Xiamen, filtered through 0.22 μm polycarbonate membranes (Millipore, USA), and stored at 4 °C. To isolate phages, filtered water samples were added to early logarithmic-phase *V. campbellii* cultures followed by incubation at 28 °C with shaking for 24 h. After removing the bacteria by filtration, the samples were diluted in SM buffer (8 mM $MgSO_4$, 50 mM Tris-HCl, 100 mM NaCl, and 0.01% (w/v) gelatin, pH 7.5), and the phages were isolated using the double-layer agar plate method. The phages were purified five times until a uniform morphology was achieved and stored in SM buffer at 4 °C in the dark [24].

Phage amplification and enrichment

The purified phage (1 mL) was added to 50 mL of early log phase host bacteria and incubated until lysis occurred. The mixture was centrifuged at 10,000 × g for 15 min at 4 °C, and the supernatant was filtered through a 0.22 μm filter. This procedure was repeated by scaling up the culture volume to 1 L. In the 1 L culture, DNase I and RNase A were added at a final concentration of 1 μg mL^{-1} each and incubated at 4 °C for 1 h. NaCl was then added (final concentration 1 mol L^{-1}), followed by incubation at 4 °C for 1 h. After centrifugation at 10,000 × g for 15 min at 4 °C, the supernatant was filtered. To the filtrate, 10% (wt vol^{-1}) polyethylene glycol 8000 was added and incubated at 4 °C for 1–3 days. The mixture was centrifuged at 12,000 × g for 15 min at 4 °C, and the pellet was resuspended in 6 mL of SM buffer. The phage suspension was purified using CsCl density gradient ultracentrifugation at 200,000 × g for 24 h at 4 °C. The concentrated phage band was extracted, dialysed using a 30 kDa ultrafiltration tube and stored in SM buffer at 4 °C in the dark.

Phage morphology observation

Phage morphology was observed using transmission electron microscopy (TEM) with phosphotungstic acid-negative staining [25]. A 10 μL drop of phage concentrate (10^{10} PFU mL^{-1}) was placed onto a carbon-coated copper grid (200 mesh) and allowed to adsorb in the dark for 10–30 min. The samples were stained with 1% phosphotungstic acid for approximately 20 min and air-dried for 30 min. The samples were observed using a JEM 2100 transmission electron microscope (Japan Electron Optics Laboratory Co., Tokyo, Japan) at 120 kV, and images were captured using a GATAN INC CCD imaging system.

Lipid test

To assess lipid presence in the phage capsid, 1 mL of phage solution (10^8 PFU mL^{-1}) was mixed with chloroform at final concentrations of 0%, 2%, and 20%. The mixture was vortexed for 30 S and incubated at 30 °C in the dark for 30 min. After low-speed centrifugation (5,000 × g, 4 °C, 5 min), 2 μL of the supernatant was placed on a *V. campbellii* LMG 11216^T agar plate. The plates were incubated at 30 °C, and plaque formation was observed. Each treatment was performed in triplicate, and SM buffer was used as a negative control.

One-step growth curve

A one-step growth curve was plotted to evaluate the infection, replication, and lysis kinetics of the phages. The host bacterium *V. campbellii* LMG 11216^T was inoculated at a 1:50 ratio into 2216E liquid medium and incubated at 160 rpm min^{-1} and 30 °C until it reached the early logarithmic phase (OD_{600} = 0.1–0.2). Phages were added to the bacterial culture at a multiplicity of infection (MOI) of 0.01. After a 5-min adsorption period in the dark, the mixture was centrifuged at 8,000 × g for 4 min at 4 °C to remove the supernatant. The resulting pellet was resuspended in 1 mL 2216E liquid medium, and this centrifugation process was repeated twice to eliminate unbound phages. The final 1 mL suspension was added to 50 mL of 2216E liquid medium and incubated at 160 rpm min^{-1} and 30 °C. Phage infectivity was measured at 10-min intervals over a 1-h period. Each treatment was conducted in triplicates.

Determination of host range

To determine the host lysis spectrum of phages R24D and R25D and compare their host range differences, a total of 57 *Vibrio* strains were selected for the experiment. These included 6 strains of *V. campbellii*, 6 strains of *V. harveyi*, 2 strains of *V. owensii*, 28 strains of *V. alginolyticus*, 9 strains of *V. parahaemolyticus*, 1 strain of *V. anguillarum*, 1 strain of *V. fluvius*, 1 strain of *V. brasiliensis*, 1 strain of *V. hepatarius*, 1 strain of *V. neocaledonicus*, and 1 strain of *V. plantisponsor*, some of which were isolated from the hepatopancreas of shrimp. The host range was assessed using a spot assay. *Vibrio* cultures of 1 mL in the early logarithmic growth phase were mixed with 5 mL of molten 2216E semisolid medium, poured onto 2216E solid agar plates, and allowed to solidify. Next, 2 μL of phage solution (containing approximately 10^8 PFU mL^{-1}) was spotted onto the solidified bacterial lawn and left to cool before incubation at 30 °C. Plaque formation was observed. Each treatment was performed in triplicate, with the host bacterium *V. campbellii* LMG 11216^T and SM buffer as the positive and negative controls, respectively.

DNA extraction and phage genome sequencing

Phage DNA was extracted using the phenol-chloroform method [25]. To the concentrated phage suspension, 1.5 μL of 100 mg mL^{-1} proteinase K solution, 100 μL of 10% sodium dodecyl sulfate solution, and 10 μL of 0.5 mol L^{-1} ethylene diamine tetraacetic acid (EDTA) were added. The mixture was incubated in a water bath at 55 °C for 3 h. After digestion, an equal volume of phenol-chloroform-isoamyl alcohol (25:24:1) was added, thoroughly mixed, and centrifuged at 12,000 × g for 5 min at 4 °C. The aqueous phase was carefully transferred to a new tube, and this step was repeated twice. The collected aqueous phase was then mixed with an equal volume of chloroform-isoamyl alcohol (24:1), shaken for 30 s, and centrifuged again at 12,000 × g for 5 min at 4 °C. The resulting aqueous phase was mixed with an equal volume of isopropanol and incubated at -20 °C for at least 1 h before centrifugation at 12,000 × g for 5 min at 4 °C. The resulting phage DNA pellet was washed twice with pre-cooled 70% ethanol, air-dried, and dissolved in 100 μL of Tris-EDTA buffer (10 mmol L^{-1} Tris-HCl, 1 mmol L^{-1} EDTA, pH 8.0), and stored at -20 °C. Complete genome sequencing of phages was performed by Hanyu Bio-Tech (Shanghai, China). The sequencing library was prepared using the NEBNext® Ultra™ DNA Library Prep Kit (NEB, USA) and sequenced on the Illumina HiSeq 4000 platform.

Phage genome analysis

Phage genome analysis was conducted using Trimmomatic v0.32 for raw data processing and Velvet v1.2.03 for genome assembly. The DNA packaging mechanism and terminal sequences of the phage genome were identified using PhageTerm on the Galaxy server (https://galaxy.pasteur.fr/). Putative open reading frames (ORFs) in the phage genome were predicted using GeneMarkS, which is available on the same platform. Each translated ORF was annotated and functionally analysed through BLASTP searches against the National Centre for Biotechnology Information (NCBI) non-redundant protein database, with an E-value threshold of $< 10^{-5}$. Transfer RNAs (tRNAs) were identified using tRNAscan-SE v.2.0 (http://lowelab.ucsc.edu/tRNAscan-SE/). Virulence genes were detected using the Virulence Factor Database (http://www.mgc.ac.cn/VFs/main.html), and antibiotic resistance genes were identified using the Comprehensive Antibiotic Resistance Database (https://card.mcmaster.ca/analyze/rgi). The lifestyles of the phages were predicted using the Phage AI platform based on the complete phage genome.

Phylogenetic and taxonomic analysis

BLASTn (http://blast.ncbi.nlm.nih.gov/Blast.cgi) was used to identify phages with the highest genomic similarity. The corresponding sequences were downloaded from GenBank (http://www.ncbi.nlm.nih.gov) and aligned using Clinker (Gilchrist, 2021) for comparative genomic analysis. Phylogenetic relationships were analysed using the VICTOR online tool (https://ggdc.dsmz.de/victor.php), which constructs viral classification and evolutionary trees. Additionally, genome similarity among the phages was assessed using the default parameters of the Virus Intergenomic Distance Calculator (VIRIDIC, https://rhea.icbm.uni-oldenburg.de/VIRIDIC/).

Determination of lytic activity

To evaluate the lytic activity of the two phages against *V. campbellii* LMG 11216^T, phage lytic assays were performed at various MOI. *V. campbellii* LMG 11216^T was inoculated into 2216E liquid medium at a 1:50 ratio and grown to the logarithmic phase (OD_{600} = 0.1–0.2) at 160 rpm min^{-1} and 30 °C. Phages were added to achieve MOI values of 0.001, 0.01, 0.1, 1, and 10. The phage-host mixtures were incubated, and bacterial growth was monitored in real-time using a Synergy H1 Multi-Mode Microplate Reader (Bio-Tek, USA) at 600 nm for 24 h. Absorbance was measured every 30 min with a pre-measurement shaking of 5 S at a temperature of 28 °C. Each condition was tested using at least five replicates, with the 2216E medium and bacterial culture serving as negative and positive controls, respectively.

Thermal stability and pH sensitivity

To assess phage resilience to environmental stress, thermal stability and pH sensitivity of the phages were tested. Phage solutions with a concentration of 10^8 PFU mL^{-1} were prepared in SM buffer. The solutions were incubated in the dark at various temperatures (4 °C, 15 °C, 25 °C, 35 °C, 45 °C, 55 °C, 65 °C, and 75 °C) for 6 h. At room temperature, the phage infectivity was measured using the double-layer agar method. To determine pH sensitivity, phage solutions were incubated in SM buffers with pH values of 2–13 at room temperature in the dark for 6 h. Phage infectivity was assessed using the double-layer agar method. Each condition was tested in triplicates. The data were analyzed using SPSS 21.0 statistical software, and all values are expressed as mean ± standard deviation (SD). Statistical differences between treatments were assessed using one-way analysis of variance (One-Way ANOVA) and Duncan's multiple range test, with a significance level set at $P < 0.05$. Graphs were created using Origin 2024 software.

Results

Phage morphological characteristics

In this study, phages vB_VcaP_R24D and vB_VcaP_R25D (hereafter referred to as R24D and R25D) were isolated

from seafood farm wastewater samples collected at the Xiashang Seafood Market and Bashi Seafood Market, Xiamen, China, using *V. campbellii* LMG 11216^{T} as the host. Both phages produced clear circular plaques, visible within approximately 4 h, with a diameter of approximately 1 mm. Over time, the plaques expanded, with R24D achieving a final diameter of 4–5 mm at an expansion rate of approximately 0.2 mm h^{-1} over 24 h. R25D plaques were slightly smaller, with a final diameter of 3–4 mm and an expansion rate of approximately 0.15 mm h^{-1} over 24 h. The plaques were clear with a surrounding translucent halo, indicating strong lytic activity (Fig. 1A). The results of the TEM analysis showed that both R24D and R25D are podoviruses, consisting of an icosahedral head (R24D: 60 ± 2.87 nm long and 69 ± 1.23 nm wide; R25D: 58 ± 2.67 nm long and 57 ± 2.16 nm wide) and a short, non-contractile tail with abundant tail fibres (Fig. 1B). Chloroform sensitivity tests revealed no significant differences in plaque morphology, size, or clarity across various chloroform concentrations. These indicate that both phages are chloroform-resistant and lack lipid-containing structures in their capsids.

One-step growth curve

The one-step growth curves revealed that both phages had a latency period of >10 min, indicating that they achieved complete replication and assembly within the host cells quickly to rapidly lyse them (Fig. 2). During the release phase, the progeny phage particles of R24D (32 ± 2 PFU $cell^{-1}$) were consistently higher than those of R25D

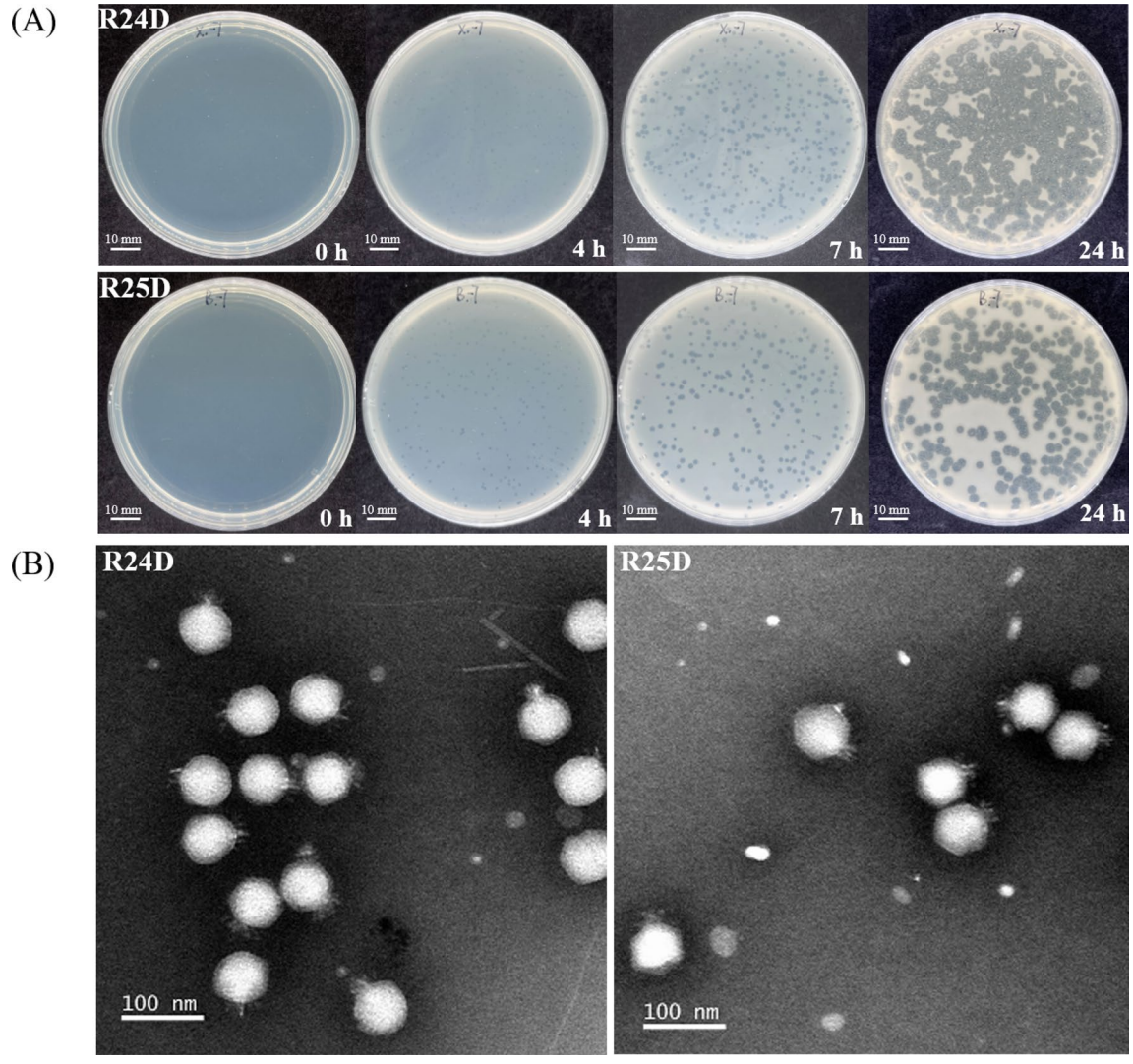

Fig. 1 Morphological characteristics of phages R24D and R25D. (**A**) Time-course images showing plaque development of phages R24D and R25D on *Vibrio* cultures at different time points (0 h, 4 h, 7 h, and 24 h). Scale bar, 10 mm; (**B**) Transmission electron microscopy images of phages R24D and R25D. Phage R24D measures 60 ± 2.87 nm in length and 69 ± 1.23 nm in width, while phage R25D measures 58 ± 2.67 nm in length and 57 ± 2.16 nm in width. Both phages exhibit a short, non-contractile tail. Scale bar, 100 nm

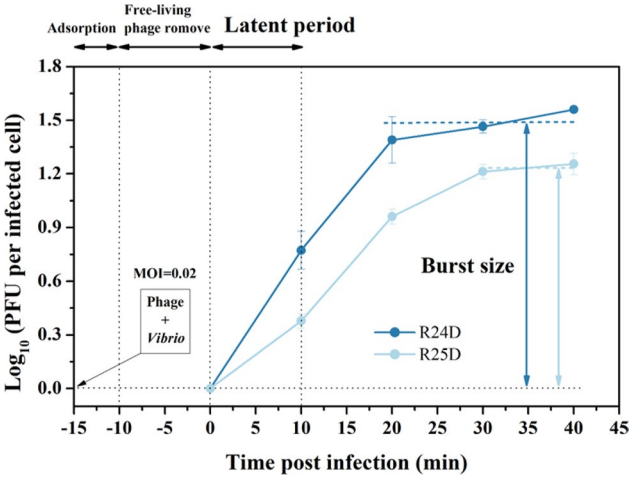

Fig. 2 One-step growth curves of phages R24D and R25D. Each data point represents the mean ± standard error of three biological replicates

(17 ± 1 PFU cell^{-1}) ($P < 0.01$), with R24D's lytic capacity nearly twice that of R25D. Summarily, both phages exhibited a short latency period and a low burst size strategy, with R24D demonstrating higher lytic activity than R25D.

Host range

The host range tests in this study included various *Vibrio* species commonly found in aquaculture environments, such as *V. campbellii*, *V. alginolyticus*, *V. parahaemolyticus*, *V. harveyi*, *V. anguillarum*, *V. owensii*, *V. brasilensis*, *V. fluvialis*, *V. hepatarius*, *V. neocaledonicus*, and *V. plantisponsor*, covering different habitats such as aquaculture water and fish tissues. The results of host range testing indicated that both phages R24D and R25D exhibited a narrow lytic range, primarily infecting the isolated host *V. campbellii* LMG 11216^{T}, demonstrating strong host specificity for both phages (see additional file 1). However, this study could not rule out the possibility that these two phages could infect other untested hosts.

Genomic features of the phages

Phages R24D and R25D possessed linear double-stranded DNA genomes, with total lengths of 44,258 bp and 43,376 bp and G + C contents of 43.69% and 43.74%, respectively. PhageTerm analysis indicated that both phages utilize the Cohesive End Sites packaging strategy, with R24D exhibiting a direct terminal repeat of 357 bp and R25D showing a direct terminal repeat of 334 bp. The ORF prediction conducted using GeneMarkS revealed that R24D contained 51 ORFs, with only the first ORF located on the negative strand and the remaining 50 on the positive strand. BLAST analysis annotated 24 of these ORFs (47.05%) based on their predicted functions. In contrast, R25D comprised 48 ORFs, all situated on the positive strand, with 22 ORFs (45.83%) annotated with predicted functions (see additional file 2). The annotated genes of both phages were categorised into functional groups, including structural proteins, DNA metabolism, DNA assembly, host lysis, and auxiliary metabolism-related genes, whereas the remaining genes were classified as hypothetical proteins (Fig. 3). Notably, none of the phages contained tRNA, virulence factors, or antibiotic resistance-related genes.

Through comparative analysis of the functional genes of the two phage strains, we identified specific similarities and differences between them. Approximately 26% of annotated functional genes were associated with DNA metabolism. These include genes encoding proteins such as T7-like RNA polymerase, RecA-like helicase (related to *Escherichia coli* bacteriophage T7 Gp4D

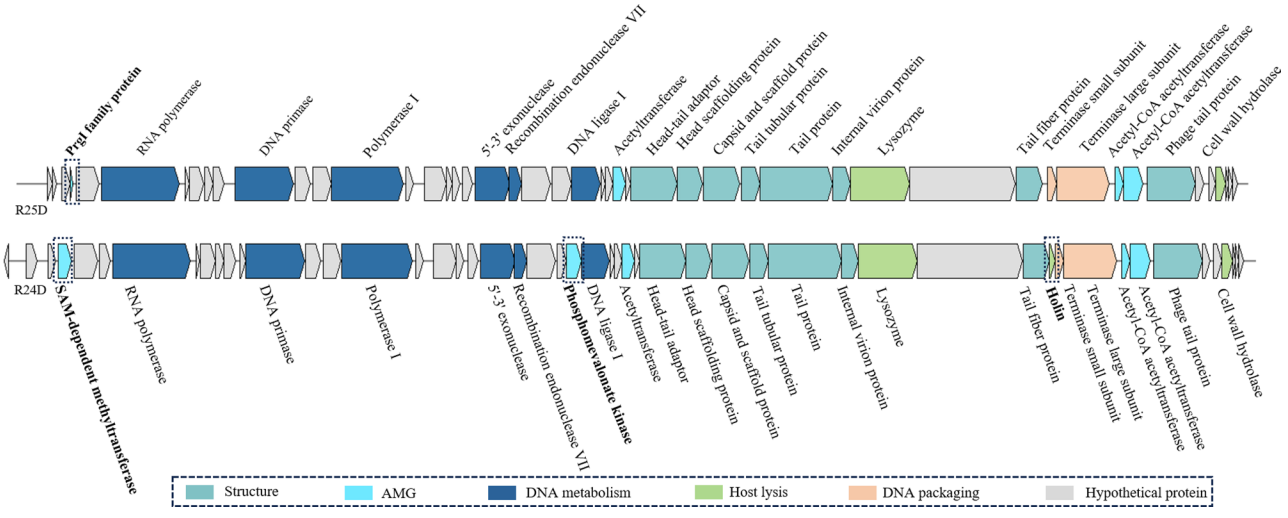

Fig. 3 Complete genomic maps of phages R24D and R25D. ORFs are depicted by arrows indicating the direction of transcription, with different functional categories color-coded, as shown at the bottom. The map was depicted using Operon software. Differential genes are highlighted within the dashed boxes. ORFs, open reading frames

helicase), DNA polymerase I, DNA ligase, 5'-3' exonuclease, and endonuclease VII. Approximately 50% of the genes were associated with structural and assembly functions, including various structural proteins such as head-tail connecting protein, head scaffolding protein, capsid and scaffold protein, tail tubular protein, tail protein, internal virion protein, and tail fibre protein. Most of these structural genes were related to the tail structure of phages. Regarding host lysis, both phages contained genes encoding cell-wall hydrolases, specifically ORF 48 in R24D and ORF 45 in R25D. Both genomes include a 699 bp gene that encodes a protein with a lysozyme domain (ORF 37 of R24D, ORF 35 of R25D). Additionally, the genomes featured auxiliary metabolic genes associated with host metabolism, including proteins from the acetyltransferase (GNAT) family and acetyl-CoA acetyltransferase (R24D: ORF 29, ORF 43, and ORF 44; R25D: ORF 27, ORF 40, and ORF 41). Phage R25D possesses a unique functional gene predicted to encode a PrgI family protein (ORF 4). In contrast, R24D contains three unique functional genes (ORF 4, ORF 25, and ORF 40) annotated as SAM-dependent methyltransferases, phosphomevalonate kinases, and holins.

Phylogenetic and taxonomic analysis

Based on NCBI BLASTN analysis, 11 phages showed high sequence identity with R24D and R25D (see additional file 3). Notably, the *V. alginolyticus* phage VEN, isolated from Greece (GenBank accession number NC_047903.1), exhibited the highest similarity to R24D and R25D, with sequence identities of 92.32% and 92.17%, and coverage rates of 85% and 88%, respectively. Phylogenetic analysis using VICTOR further confirmed that R24D, R25D, and VEN clustered together, indicating a close evolutionary relationship among the three phages (Fig. 4A). All three phages were isolated from environments associated with aquaculture and seafood sales, with the difference being that the hosts for phages R24D and R25D were *V. campbellii*, and the host for phage VEN was *V. alginolyticus* (Fig. 4A). Genomic similarity analysis using VIRIDIC revealed that R24D and R25D had 80.4% and 82.9% intergenomic similarity with VEN, respectively, whereas the similarity between R24D and R25D was

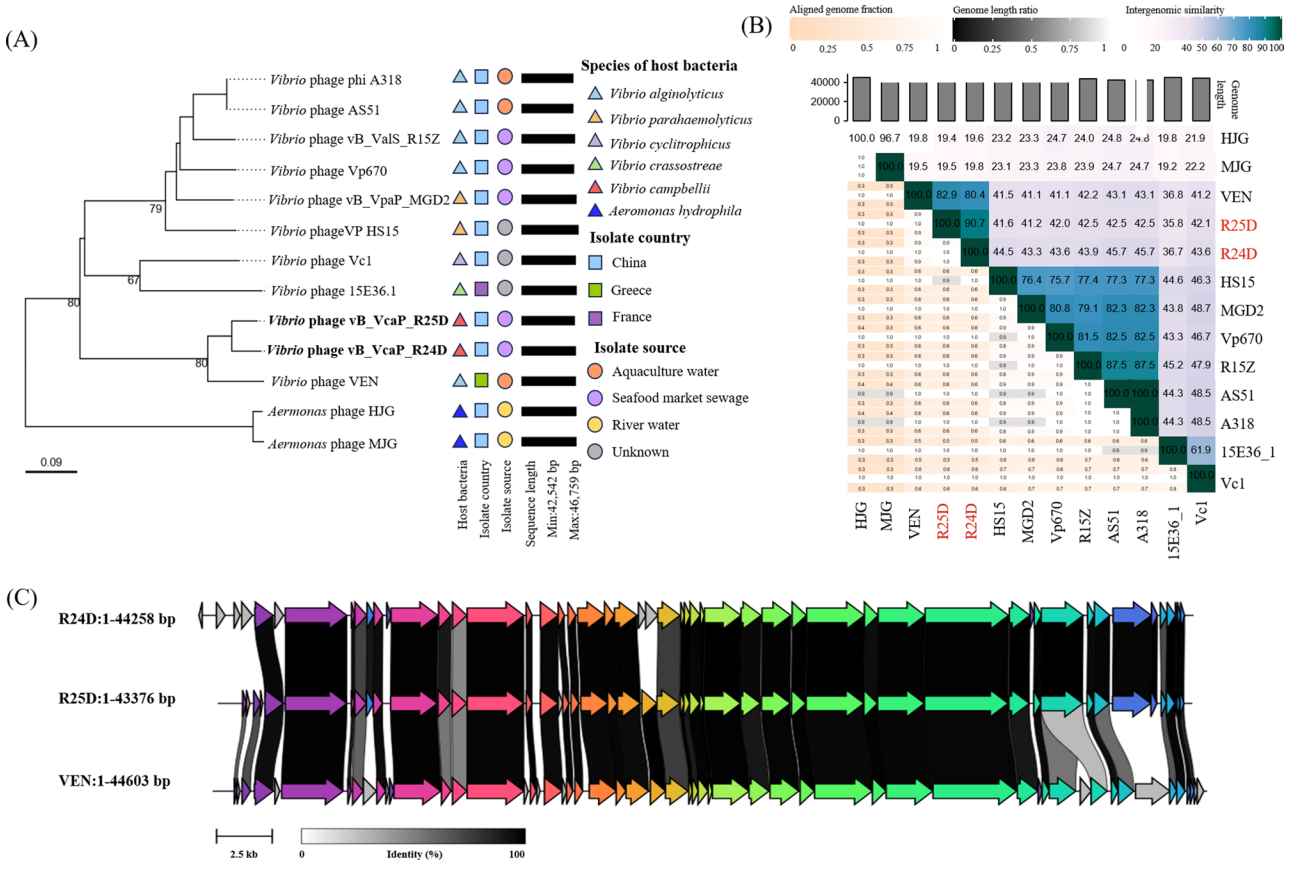

Fig. 4 Phylogenetic analysis and whole-genome comparison of phages. (**A**) A phylogenetic tree illustrating the relationship between R24D, R25D, and other closely related phages, constructed using the VICTOR web service; (**B**) A heatmap displaying pairwise intergenomic distances between each pair of phages, constructed using the VIRDIC web service. (**C**) Comprehensive genomic comparisons among R24D, R25D, and VEN using Clinker. ORFs with high similarities are denoted by arrows of the same colour, with the darkness of blocks representing the degree of similarity. ORFs, open reading frames

90.7%. This indicates that all three phages belong to the genus *Trungvirus* within the family *Autographiviridae* (intergenomic similarity > 75%) but represent different species within this genus (intergenomic similarity < 95%) (Fig. 4B). Comparative genomic analysis of the whole genomes of phages R24D, R25D, and VEN revealed that their genomes could be divided into functional categories related to structural proteins, DNA metabolism, DNA assembly, host lysis, and auxiliary metabolism. The genes associated with DNA metabolism and tail structure proteins showed high homology among the three phages (91.58–99.45%) (Fig. 4C).

Comparative whole-genome analysis of the closely related phages R24D, R25D, and VEN revealed a high degree of sequence homology in genes encoding RNA polymerase, DNA primase, DNA polymerase, 5'-3' exonuclease, and recombination endonuclease VII, suggesting that these phages share conserved DNA metabolism processes and pathways. Furthermore, genes associated with the head-tail connecting protein and tail tubular protein exhibited significant homology across all three phages, indicating structural similarities in their tail assemblies. All three phages harboured genes encoding cell wall hydrolases and lysozyme domain-containing proteins, supporting their classification as virulent. Notably, a gene encoding holin was identified in the genomes of R24D and VEN, whereas it was absent in the corresponding genomic region of R25D.

Lytic activity

The lytic activities of phages R24D and R25D against the host *V. campbellii* LMG 11216^T under different MOI conditions are shown in Fig. 5. After adding phages R24D, R25D, or their mixture to the host bacterial

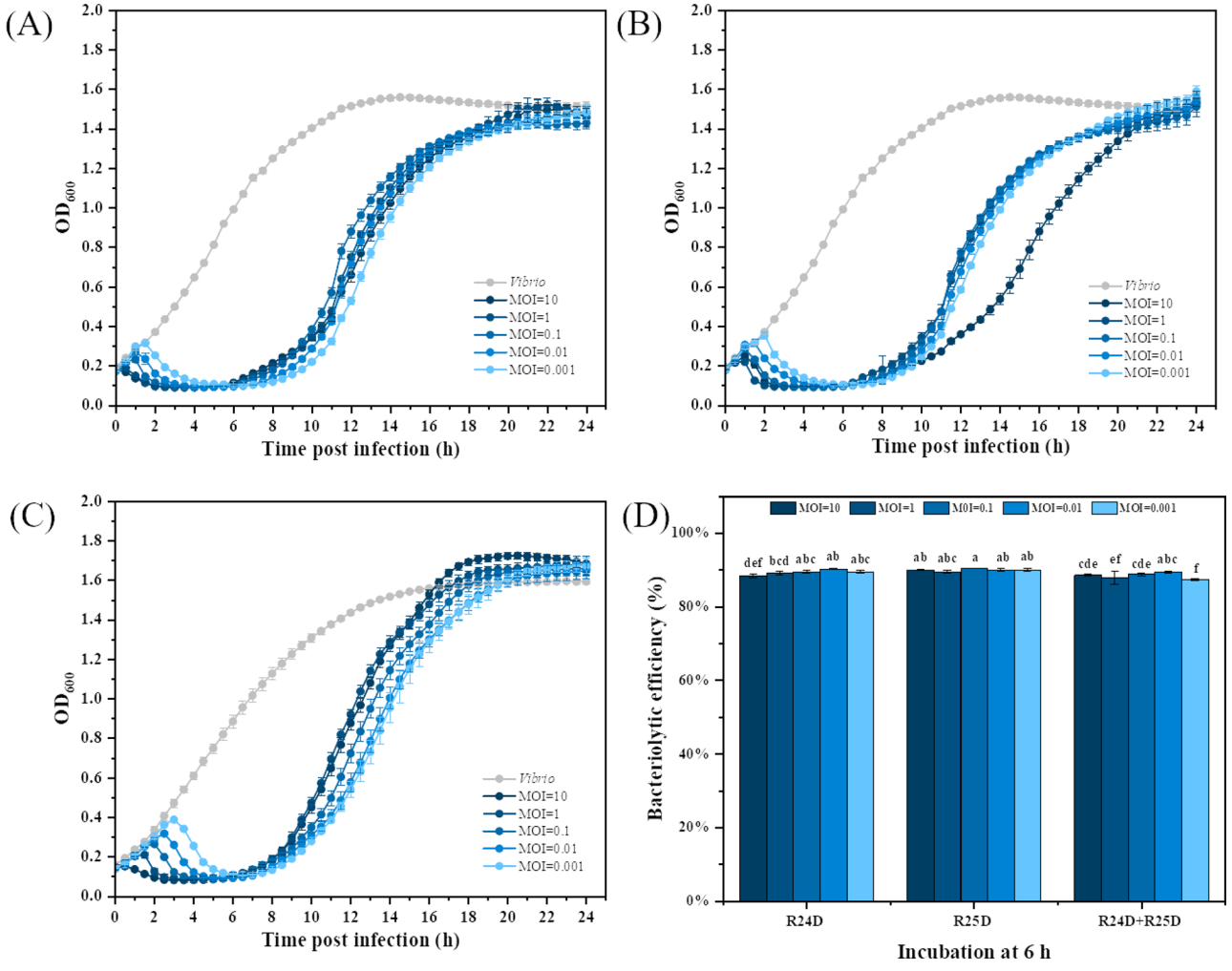

Fig. 5 Bactericidal effects of R24D and R25D. (**A**) Lytic activity of R24D against *V. campbellii* LMG 11216^T at various MOIs over 24 h, with measurements taken at 30-min intervals. (**B**) Lytic activity of R25D against *V. campbellii* LMG 11216^T at various MOIs over 24 h, with measurements taken at 30-min intervals. (**C**) Lytic activity of a 1:1 mixture of R24D and R25D against *V. campbellii* LMG 11216^T at various MOIs over 24 h, with measurements taken at 30-min intervals. (**D**) Lysis efficiency after 6 h of co-culture in different systems. Each treatment was conducted with six replicates, and the data are presented as the mean ± standard deviation. MOIs, multiplicity of infection

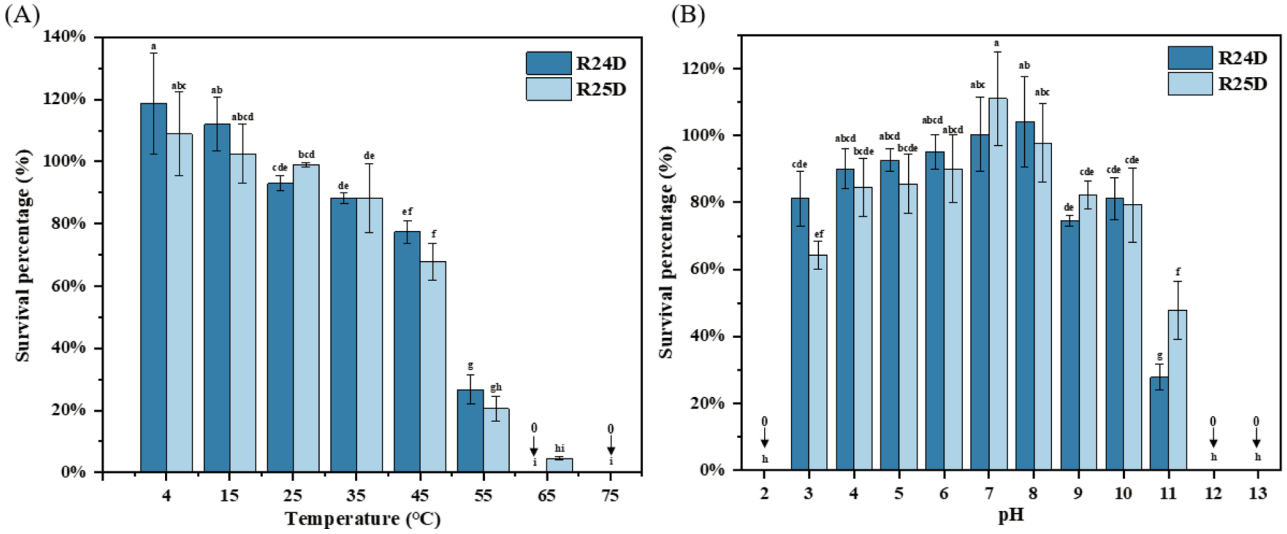

Fig. 6 Environmental stability of phages. (**A**) Survival rates of phages R24D and R25D under temperature conditions ranging from 4 °C to 75 °C; (**B**) Survival rates of phages R24D and R25D at pH levels ranging from 2 to 13. Each data point represents the mean ± standard error of three biological replicates

culture during the exponential growth phase, all treatments rapidly lysed the host cells. Higher MOI levels correlated with a stronger lytic effect, effectively maintaining the OD_{600} of the host bacteria below 0.4 during the initial incubation phase (Fig. 5A–C). After 6 h of co-culturing, the lytic effects of phages R24D and R25D and the phage mixture on the growth of host bacteria peaked, with a bactericidal efficiency of approximately 90% under all MOI conditions tested (MOI ranging from 0.001 to 10) (Fig. 5D). Further analysis revealed that at MOIs of 0.001–0.1, phages R24D and R25D exhibited slightly higher bactericidal efficiency compared with higher MOIs (0.1–10), indicating that a small amount of R24D could achieve a significant bactericidal effect quickly. Notably, when both phages were mixed and added to the host during the exponential growth phase, the lytic effect was not significantly different from that of the individual phages, suggesting that combining these two phages did not enhance their overall bactericidal efficiency.

Thermal stability and pH sensitivity

The environmental stability results for phages R24D and R25D are shown in Fig. 6. For thermal stability, both phages maintained high activity (survival rate > 90%) within the temperature range of 4–35 °C. Their activity significantly decreased at 55 °C (Fig. 6A). Phage R24D became completely inactive at 65 °C, whereas phage R25D retained some activity (survival rate > 4.5%) at 65 °C and only became completely inactive at 75 °C. Overall, phages R24D and R25D exhibited good stability within the temperature range of 4 °C to 45 °C. However, R24D exhibited an increased sensitivity to high temperatures and was more susceptible to temperature fluctuations than R25D. For pH sensitivity, both phages showed optimal stability between pH 7 and 8, with survival rates ranging from 95.56 to 111.1%. They remained highly active (survival rate > 80%) in the pH range of 4–10 but completely lost activity at a pH of < 3 or > 11. Data analysis revealed no significant difference in survival rates between the two phages within the pH range of 3–10. However, at pH 11, the survival rate of R25D was significantly higher than that of R24D ($P < 0.05$), indicating that R25D has a stronger tolerance to alkaline conditions.

Discussion

The high organic content and suitable temperature in seafood market wastewater and sewage create favourable conditions for *Vibrio* colonisation, resulting in a high abundance of these bacteria. This rich nutritional environment and high *Vibrio* density contribute to the high abundance and easy isolation of vibriophages [26]. In this study, two virulent phages, vB_VcaP_R24D and vB_VcaP_R25D, were isolated from aquaculture wastewater from a seafood market in Xiamen, China, using *V. campbellii* LMG 11216^T as a host. Both phages rapidly produced clear plaques, with only a few resistant *Vibrio* cells remaining unlysed, indicating a strong lytic ability against the host [27]. Genomic analysis has revealed that both R24D and R25D possess genes encoding lysozymes (ORF 37 of R24D and ORF 35 of R25D) and cell wall hydrolases (ORF 48 of R24D and ORF 45 of R25D), enabling phages to effectively degrade the *Vibrio* cell wall and facilitate infection and lysis [28]. Furthermore, the absence of lysogenic genes for both phages, indicates that they did not enter the lysogenic cycle during infection. Instead, lytic genes ensure efficient host lysis, thereby reducing the risk of horizontal gene transfer. Predictions derived from Phage AI software also confirmed that both phages had

100% lytic potential. The lytic capability of these phages is a prerequisite for their application in disease treatment. When applied in phage therapy, highly lytic phages can rapidly and effectively kill host bacteria, control pathogen populations, limit the spread of infections, and accelerate pathogen clearance. In contrast to lysogenic phages, purely lytic phages reduce the likelihood of resistance mutations, provide more effective pathogen control, lower the risk of resistance, and significantly improve the therapeutic outcomes in aquaculture environments [29].

Both phages showed a short latent period and a small burst size, which aligned with the "Fast-low strategy" in the *r*-strategy [30]. Such phages exhibit a rapid lifecycle and low reproductive output, leading to the rapid lysis of host cells during infection. Because of small burst size, they possess strong local infectivity without extensive dissemination, thereby restricting the development of phage mutations and bacterial resistance. Phages with the "Fast-low strategy" have significant application potential in rapidly mitigating the pathogens without inducing excessive immune responses or disrupting the stability of existing microbial communities [31, 32]. Numerous studies have identified phages with short latent periods and small burst sizes. For instance, *V. parahaemolyticus* phage R16F has a latent period of > 10 min and a burst size of 13 PFU cell^{-1} [33]. Six *V. parahaemolyticus* phages isolated from seafood samples by Tan et al. exhibited short latent periods and small burst sizes, with latent periods ranging from 10 to 20 min and burst sizes ranging between 17 and 51 PFU cell^{-1} [34]. Phages R24D and R25D have relatively small genomes (44,258 bp for R24D and 43,376 bp, for R25D) and contain genes encoding lysozymes and cell wall hydrolytic enzymes, as well as a rich array of tail proteins. Previous studies indicated that highly specific tail fibres can rapidly recognise and bind to host bacterial receptors while puncturing proteins or tail spike structures that swiftly penetrate the cell wall to inject phage DNA. The diversity and functionality of tail proteins ensure precise DNA injection, and the smaller genome size shortens the time required for phage DNA injection into the host cell as well as for the production and assembly of progeny phage DNA. Efficient host recognition, rapid cell penetration, and synergistic action with lytic proteins ultimately accelerate the lysis process [35, 36]. The strategy of short latent periods and small burst sizes enables phages to rapidly lyse pathogenic bacteria within a short timeframe, showing a strong application potential for aquaculture environments where vibriosis is prevalent, particularly in high-density *Vibrio* environments. This approach can rapidly control pathogen abundance and prevent disease spread [37]. Although the two bacteriophages have a narrow host range, this characteristic can also minimize off-target effects on beneficial microbial communities in aquaculture environments, thereby preserving beneficial microbial communities.

According to the whole-genome comparative analysis, the three unique functional genes (ORF4, ORF25, and ORF40) found in R24D may play a significant role in its higher burst size and larger plaque. ORF4 has been annotated as a S-adenosyl-L- methionine-dependent methyltransferase involved in DNA modification processes, particularly methylation. This function helps the phage resist the restriction modification system of the host cell by protecting its genome from degradation, thus enabling R24D to maintain higher levels of phage production [38]. ORF25 was annotated as a phosphomevalonate kinase, an enzyme associated with the isoprenoid biosynthetic pathway. This enzyme is involved in the production of the phage envelope components and other molecular precursors. By enhancing the synthesis efficiency of lipids and small molecules, ORF25 may optimise the assembly efficiency of structural proteins and the formation of phage particles, thereby increasing burst size. Such metabolic advantage would likely allow R24D to produce more progeny phages within a shorter period [39]. ORF 40 is annotated as holins, which form pores in the cell membrane, allowing lysozymes (such as endolysins) to pass through the membrane into the periplasmic space, where they degrade the cell wall, ultimately leading to cell lysis and promoting the release of progeny phages [40]. Plaque formation can be viewed as a competition between bacteriophage-induced bacterial lysis and bacterial lawn development. Several factors can contribute to larger plaque formation. For example, a higher burst size would promote a more effective infection and lysis of bacteria, leading to accelerated plaque growth [41]. Phage R24D's higher burst size than R25D is likely responsible for its larger plaques. Summarily, the unique genomic features of R24D, particularly the presence of methyltransferases, phosphomevalonate kinases, and holin, enhanced genome protection, metabolic efficiency, and infection efficiency, thereby promoting higher progeny phage production and plaque expansion, resulting in a significantly larger burst size and slightly larger plaques than those in R25D [27, 42].

Assessing the genetic safety of vibriophages is a crucial prerequisite for their use in aquaculture to treat vibriosis. Genetic safety not only impacts the effectiveness of phage therapy but also concerns the environmental health and cultured organisms. The genomes of vibriophages used in aquaculture do not contain any toxin genes or pathogenic factors that could be harmful to aquatic animals to prevent severe toxicity in cultured species if toxins are released into the aquatic environment. Additionally, phage genomes should not harbour antibiotic resistance genes (ARGs) to avoid enhancing the antibiotic resistance of pathogenic bacteria during treatment. Furthermore,

phages should not carry integrative genetic elements, such as integrase genes or transposons, which can facilitate the integration of phage genes into the host bacterial genome, potentially increasing genetic variation in the host bacteria and promoting horizontal gene transfer, thereby posing an evolutionary risk to pathogens [29, 43]. Genomic analysis indicated that neither R24D nor R25D contained virulence factors, ARGs, or integrative genetic elements, such as integrases, suggesting that these phages have promising genetic safety profiles for application.

The lysis curves demonstrated the significant potential of these phages for use in aquaculture to treat vibriosis. Both phages exhibited strong lytic activity against *Vibrio* hosts, making them suitable for phage therapy. They effectively control the abundance of *Vibrio* in the early stages, providing a means to prevent and manage vibriosis [44]. The phages showed the highest lytic efficiency when co-cultured with the host *Vibrio* for 6 h, achieving up to 90% lysis at various MOIs. Additionally, the short latent period of these phages allowed them to significantly suppress the growth of *Vibrio* during the logarithmic phase, maintaining the OD_{600} of the host *Vibrio* below 0.4. Efficient lysis offers a clear advantage for preventing vibriosis. In laboratory studies with pure strains, although phage-resistant *Vibrio* can re-grow in later culture stages, other microbial populations or probiotics can replace the resistant strains and become dominant. Therefore, the combined use of phages and probiotics should be considered as a strategy for effective microbial control in aquaculture systems. Phages R24D and R25D did not show significant synergistic effects in the mixed systems, likely because of their similar biological characteristics, causing competition between the two phages. Given the narrow host range of the phages, combining these two phages with other complementary phages could potentially broaden their lytic range and enhance their overall application potential. These findings offer valuable insights for future researches on phage cocktail formulations for *Vibrio* control, emphasising the need to consider interactions and synergistic dynamics among phages when designing phage cocktails. Cocktails containing phages with diverse life histories, infection strategies, and host lysis profiles should be prioritized to optimize host control. For instance, combining a phage with a rapid lysis cycle and one with a longer latent period but strong diffusion capability can achieve both rapid infection control and sustained long-term protection [45–48].

The temperature stability and pH tolerance results indicated that both phages have good stability in aquaculture environments. Both phages maintain high activity (survival rate > 90%) below 35 °C and only become completely inactive at temperatures above 55–65 °C. They also exhibited activity over a broad pH range of 3–11, with optimal pH levels between 7 and 8. Interestingly, R24D exhibited higher sensitivity to thermal stress (65 °C) and alkaline conditions (pH 11) compared to R25D. Genomic analysis revealed that R24D harbors a unique SAM-dependent methyltransferase gene (ORF4), which is involved in the modification of nucleic acids or proteins. This enzyme may influence the stability of structural components such as the phage capsid or tail proteins, potentially making R24D more vulnerable to degradation under extreme conditions. In contrast, R25D possesses a unique gene encoding a PrgI family protein (ORF4), which is typically involved in stabilizing membrane-associated proteins and may confer additional structural robustness to R25D. These findings suggest that the genomic differences between R24D and R25D may contribute to their distinct environmental resilience. Further studies, such as protein structure and expression analyses, are warranted to confirm these hypotheses.

Before using these phages in aquaculture, it is important to consider factors such as the preparation process, storage conditions, transportation, and environmental conditions during use. High environmental temperatures or pH fluctuations can affect phage activity and the effectiveness of phage therapy [47, 48]. The suitable temperature range for aquaculture water is between 24 °C and 30 °C, and the pH range is between 7.5 and 8.5. Furthermore, the observed stability aligns with the requirements of aquaculture across diverse geographic regions and climates. For example, in tropical aquaculture systems, water temperatures can approach the upper limits of the optimal range, while in temperate regions, seasonal variations might bring temperatures closer to the lower limits [49, 50]. Similarly, fluctuations in water quality parameters, such as pH, may occur in intensive aquaculture systems [51]. The ability of these phages to retain high activity under these variable conditions highlights their robustness and broad applicability. These findings also provide practical guidance for the production, preparation, transportation, storage, and application of these phages. Ensuring appropriate handling protocols to mitigate extreme temperature or pH conditions during storage and use will be essential for maximizing their efficacy in controlling *Vibrio* infections. This comprehensive understanding of environmental stability enhances the potential for these phages to be effectively deployed in aquaculture systems globally.

Conclusion

Vibriophages vB_VcaP_R24D and vB_VcaP_R25D exhibited significant attributes, including robust lytic activity, short latent periods, favourable genetic safety profiles, effective bactericidal action, and substantial environmental stability. These characteristics underscore their high feasibility and considerable potential for application in

treating *Vibrio* diseases in aquaculture systems. Given the diversity of *Vibrio* strains found in these environments, future research should focus on exploring the broad-spectrum lytic capabilities of these phages against various *Vibrio* strains, including additional untested strains, and developing phage cocktails. Additionally, exploring the combined use of phages with probiotics and other complementary products could further enhance therapeutic effectiveness. Long-term field trials would also be essential to validate the safety and effectiveness of these phages in aquaculture settings. This study provides strong evidence supporting the practical application of phage therapy and offers scientific guidance for developing green and sustainable aquaculture strategies, while emphasizing the need for ecological compatibility.

Abbreviations

AHPND	Acute hepatopancreatic necrosis disease
OD	Optical density
TEM	Transmission electron microscopy
MOI	Multiplicity of infection
ORFs	Open reading frames
ARGs	Antibiotic resistance genes
VIRIDIC	Virus Intergenomic Distance Calculator
NCBI	National Centre for Biotechnology Information
EDTA	Ethylene diamine tetraacetic acid
tRNAs	Transfer RNAs

Supplementary Information

The online version contains supplementary material available at https://doi.org/10.1186/s12866-025-03803-0.

Supplementary Material 1

Author contributions

All authors actively engaged in the review process and provided their approval for the manuscript. R. Z and YL. Y contributed to the administration, resources management, and funding acquisition. HY. D, YL. Y, KM. S, M. H and WQ. L were responsible for tasks related to phage isolation, conducting ecophysiological experiments and analyzing data. HY. D, YL. Y and KM. S played pivotal roles in drafting the original manuscript and creating visualizations. R. Z, YL. Y, X. L and J. X supervised the experiment and manuscript writing, contributed to conceptualization, administration and draft editing.

Funding

This study is financed by Science and Technology Development Fund ofMacau (0055/2023/RIB2), the Guangdong Major Project of Basic and Applied Basic Research (2023B0303000017), the Innovation Team Project of Universities in Guangdong Province (No. 2023KCXTD028), and the research fund from Synthetic Biology Research Center of Shenzhen University.

Data availability

The complete genome was submitted to GenBank under the accession numbers PQ464790 for R24D and PQ464789 for R25D.

Declarations

Ethics approval and consent to participate

This article does not include any studies involving humans or animals. Clinical trial number: not applicable.

Competing interests

The authors declare no competing interests.

Author details

[1]College of the Environment and Ecology, Xiamen University, Xiamen 361102, China
[2]State Key Laboratory of Marine Environmental Science, Xiamen University, Xiamen, Fujian 361102, China
[3]College of Ocean and Earth Sciences, Xiamen University, Xiamen, Fujian 361102, China
[4]Institute of Marine Biology, National Taiwan Ocean University, No.2, Pei-Ning Road, Keelung, Taiwan 20224, China
[5]Center for Regional Ocean & Department of Ocean Science and Technology, Faculty of Science and Technology, University of Macau, Taipa, Macau, China
[6]Archaeal Biology Center, Synthetic Biology Research Center, Shenzhen Key Laboratory of Marine Microbiome Engineering, Key Laboratory of Marine Microbiome Engineering of Guangdong Higher Education Institutes, Institute for Advanced Study, Shenzhen University, Shenzhen 518055, China

Received: 6 November 2024 / Accepted: 4 February 2025
Published online: 28 February 2025

References

1. Mohamad N, Amal MNA, Yasin ISM, Zamri Saad M, Nasruddin NS, Al-saari N, et al. Vibriosis in cultured marine fishes: a review. Aquaculture. 2019;512:734289.
2. Ina-Salwany MY, Al-Saari N, Mohamad A, Mursidi FA, Mohd-Aris A, Amal MNA, et al. Vibriosis in Fish: a review on Disease Development and Prevention. J Aquat Anim Health. 2019;31(1):3–22.
3. Yue K, Shen Y. An overview of disruptive technologies for aquaculture. Aquaculture Fisheries. 2022;7:111–20.
4. De Souza Valente C, Wan AHL. *Vibrio* and major commercially important vibriosis diseases in decapod crustaceans. J Invertebr Pathol. 2021;181:107527.
5. De Schryver P, Defoirdt T, Sorgeloos P. Early Mortality Syndrome outbreaks: a Microbial Management issue in shrimp farming? PLoS Pathog. 2014;10:e1003919.
6. Dong X, Song J, Chen J, Bi D, Wang W, Ren Y, et al. Conjugative transfer of the pVA1-Type plasmid carrying the *pirABvp* genes results in the formation of New AHPND-Causing Vibrio. Front Cell Infect Microbiol. 2019;9:195.
7. González-Gómez JP, Soto-Rodriguez SA, Gomez-Gil B, Serrano-Hernández JM, Lozano-Olvera R, López-Cuevas O, et al. Effect of phage therapy on survival, histopathology, and water microbiota of *Penaeus vannamei* challenged with *Vibrio parahaemolyticus* causing acute hepatopancreatic necrosis disease (AHPND). Aquaculture. 2023;576:739851.
8. Dong X, Wang H, Xie G, Zou P, Guo C, Liang Y, et al. An isolate of *Vibrio campbellii* carrying the pir^{VP} gene causes acute hepatopancreatic necrosis disease. Emerg Microbes Infections. 2017;6:1–3.
9. Haldar S, Chatterjee S, Sugimoto N, Das S, Chowdhury N, Hinenoya A, et al. Identification of *Vibrio campbellii* isolated from diseased farm-shrimps from south India and establishment of its pathogenic potential in an *Artemia* model. Microbiology. 2011;157:179–88.
10. Xiao J, Liu L, Ke Y, Li X, Liu Y, Pan Y, et al. Shrimp AHPND-causing plasmids encoding the PirAB toxins as mediated by *pirAB*-Tn903 are prevalent in various *Vibrio* species. Sci Rep. 2017;7:42177.
11. Dash P, Avunje S, Tandel RS, Panigrahi KPS. Biocontrol of luminous vibriosis in shrimp aquaculture: a review of current approaches and future perspectives. Reviews Fisheries Sci Aquaculture. 2017;25:245–55.
12. Leal JF, Santos EBH, Esteves VI. Oxytetracycline in intensive aquaculture: water quality during and after its administration, environmental fate. Toxic Bacterial Resist Reviews Aquaculture. 2019;11:1176–94.
13. Xu K, Wang Y, Yang W, Cai H, Zhang Y, Huang L. Strategies for Prevention and Control of Vibriosis in Asian Fish Culture. Vaccines. 2022;11:98.
14. Pérez-Sánchez T, Mora-Sánchez B, Balcázar JL. Biological approaches for disease control in aquaculture: advantages, limitations and challenges. Trends Microbiol. 2018;26(11):896–903.
15. Kowalska JD, Kazimierczak J, Sowińska PM, Wójcik EA, Siwicki AK, Dastych J. Growing Trend of fighting infections in aquaculture Environment—opportunities and challenges of Phage Therapy. Antibiotics. 2020;9:301.
16. Cherian T, Ragavendran C, Vijayan S, Kurien S, Peijnenburg WJGM. A review on the fate, human health and environmental impacts, as well as regulation of antibiotics used in aquaculture. Environ Adv. 2023;13:100411.

17. Abedon ST, García P, Mullany P, Aminov R. Editorial: Phage therapy: past, Present and Future. Front Microbiol. 2017;8.
18. Caflisch KM, Suh GA, Patel R. Biological challenges of phage therapy and proposed solutions: a literature review. Expert Rev Anti-infective Therapy. 2019;17:1011–41.
19. Alagappan K, Karuppiah V, Deivasigamani B. Protective effect of phages on experimental *V. parahaemolyticus* infection and immune response in shrimp (Fabricius, 1798). Aquaculture. 2016;453:86–92.
20. Xia H, Yang H, Yan N, Hou W, Wang H, Wang X, et al. Bacteriostatic effects of phage F23s1 and its endolysin on *Vibrio parahaemolyticus*. J Basic Microbiol. 2022;62:963–74.
21. Oliveira J, Castilho F, Cunha A, Pereira MJ. Bacteriophage therapy as a bacterial control strategy in aquaculture. Aquacult Int. 2012;20:879–910.
22. Stalin N, Srinivasan P. Characterization of *Vibrio parahaemolyticus* and its specific phage from shrimp pond in Palk Strait, South East coast of India. Biologicals. 2016;44:526–33.
23. Cai R, Li D, Qin W, Lin W, Pan L, Qian M, et al. A novel *Vibrio alginolyticus* phage and its therapy application in *Portunus trituberculatus* larvae. Aquaculture. 2024;579:740165.
24. Lu L, Cai L, Jiao N, Zhang R. Isolation and characterization of the first phage infecting ecologically important marine bacteria *Erythrobacter*. Virol J. 2017;14:104.
25. Yang Y, Cai L, Ma R, Xu Y, Tong Y, Huang Y, et al. A Novel Roseosiphophage isolated from the Oligotrophic South China Sea. Viruses. 2017;9:109.
26. Liang X, Wang Y, Hong B, Li Y, Ma Y, Wang J. Isolation and characterization of a Lytic *Vibrio parahaemolyticus* phage vB_VpaP_GHSM17 from sewage samples. Viruses. 2022;14:1601.
27. Abedon ST. Detection of bacteriophages: phage plaques. In: Harper DR, Abedon ST, Burrowes BH, McConville ML, editors. Bacteriophages. Cham: Springer International Publishing; 2018. pp. 1–32.
28. Daniel C, Nelson M, Schmelcher L, Rodriguez-Rubio J, Klumpp, David G, et al. Endolysins as Antimicrobials Adv Virus Res. 2012;83:299–365.
29. Guo Z. Mini review advantages and limitations of lytic phages compared with chemical antibiotics to combat bacterial infections. 2024.
30. Dickins TE, Dickins BJA. Evolutionary biology: contemporary and historical reflections upon core theory. 1st ed. Cham: Springer; 2023.
31. De Paepe M, Taddei F. Viruses' life history: towards a mechanistic basis of a Trade-Off between Survival and Reproduction among phages. PLoS Biol. 2006;4:e193.
32. Abedon ST, Hyman P, Thomas C. Experimental examination of Bacteriophage latent-period evolution as a response to bacterial availability. Appl environ microbiol. 2003;69.
33. Chen Y, Li W, Shi K, Fang Z, Yang Y, Zhang R. Isolation and characterization of a novel phage belonging to a new genus against *Vibrio parahaemolyticus*. Virol J. 2023;20:81.
34. Tan CW, Rukayadi Y, Hasan H, Abdul-Mutalib N-A, Jambari NN, Hara H, et al. Isolation and characterization of six *Vibrio parahaemolyticus* Lytic bacteriophages from Seafood samples. Front Microbiol. 2021;12:616548.
35. Kostyuchenko VA, Chipman PR, Leiman PG, Arisaka F, Mesyanzhinov VV, Rossmann MG. The tail structure of bacteriophage T4 and its mechanism of contraction. Nat Struct Mol Biol. 2005;12:810–3.
36. Cuervo A, Fàbrega-Ferrer M, Machón C, Conesa JJ, Fernández FJ, Pérez-Luque R, et al. Structures of T7 bacteriophage portal and tail suggest a viral DNA retention and ejection mechanism. Nat Commun. 2019;10:3746.
37. Gill J, Hyman P. Phage choice, isolation, and Preparation for Phage Therapy. CPB. 2010;11:2–14.
38. Guo X, Söderholm A, Kanchugal PS, Isaksen GV, Warsi O, Eckhard U, et al. Structure and mechanism of a phage-encoded SAM lyase revises catalytic function of enzyme family. eLife. 2021;10:e61818.
39. Chen Z, Zhou X, Zhou X, Tang Y, Lu M, Zhao J, et al. Phosphomevalonate Kinase Controls β-Catenin signaling via the metabolite 5-Diphosphomevalonate. Adv Sci. 2023;10:2204909.
40. Young R. Phage lysis: three steps, three choices, one outcome. J Microbiol. 2014;52:243–58.
41. Harper DR, Abedon ST, Burrowes BH, McConville ML, editors. Bacteriophages: Biology, Technology, Therapy. Cham: Springer International Publishing; 2021.
42. Longin H, Broeckaert N, Van Noort V, Lavigne R, Hendrix H. Posttranslational modifications in bacteria during phage infection. Curr Opin Microbiol. 2024;77:102425.
43. Torres-Barceló C, Turner PE, Buckling A. Mitigation of evolved bacterial resistance to phage therapy. Curr Opin Virol. 2022;53:101201.
44. Mäntynen S, Laanto E, Oksanen HM, Poranen MM, Díaz-Muñoz SL. Black box of phage–bacterium interactions: exploring alternative phage infection strategies. Open Biology. 2021;11:9.
45. Gu J, Liu X, Li Y, Han W, Lei L, Yang Y, et al. A method for generation phage cocktail with great therapeutic potential. PLoS ONE. 2012;7:e31698.
46. Benjamin K, Chan, Abedon ST, Loc-Carrillo C. Phage cocktails and the future of phage therapy. Future Microbiol. 2013;8:769–83.
47. Silva YJ, Costa L, Pereira C, Mateus C, Cunha Â, Calado R, et al. Phage therapy as an Approach to prevent *Vibrio anguillarum* infections in Fish Larvae production. PLoS ONE. 2014;9:e114197.
48. Ramos-Vivas J, Superio J, Galindo-Villegas J, Acosta F. Phage therapy as a focused management strategy in aquaculture. Int J Mol Sci. 2021;22:10436.
49. Food and Agriculture Organization of the United Nations (FAO). Climate change implications for fisheries and aquaculture: Summary. FAO Fisheries Aquaculture Tech Paper. 2020;627:1–654.
50. Food and Agriculture Organization of the United Nations (FAO). Adaptations to the climate crisis in fisheries and aquaculture. 2022.
51. Lindholm-Lehto P. Water quality monitoring in recirculating aquaculture systems. Aquaculture Fish Fisheries. 2023;3:113–31.

Publisher's note